the plant journal

SEB Society for Experimental Biology

The Plant Journal (2014) **79,** 348–359 doi: 10.1111/tpj.12554

TECHNICAL ADVANCE

Both CRISPR/Cas-based nucleases and nickases can be used efficiently for genome engineering in *Arabidopsis thaliana*

Friedrich Fauser†, Simon Schiml† and Holger Puchta*

Botanical Institute II, Karlsruhe Institute of Technology, POB 6980, 76049 Karlsruhe, Germany

Received 28 March 2014; revised 28 April 2014; accepted 6 May 2014; published online 16 May 2014.
*For correspondence (e-mail holger.puchta@kit.edu).
†These authors contributed equally to the work.

SUMMARY

Engineered nucleases can be used to induce site-specific double-strand breaks (DSBs) in plant genomes. Thus, homologous recombination (HR) can be enhanced and targeted mutagenesis can be achieved by error-prone non-homologous end-joining (NHEJ). Recently, the bacterial CRISPR/Cas9 system was used for DSB induction in plants to promote HR and NHEJ. Cas9 can also be engineered to work as a nickase inducing single-strand breaks (SSBs). Here we show that only the nuclease but not the nickase is an efficient tool for NHEJ-mediated mutagenesis in plants. We demonstrate the stable inheritance of nuclease-induced targeted mutagenesis events in the *ADH1* and *TT4* genes of *Arabidopsis thaliana* at frequencies from 2.5 up to 70.0%. Deep sequencing analysis revealed NHEJ-mediated DSB repair in about a third of all reads in T1 plants. In contrast, applying the nickase resulted in the reduction of mutation frequency by at least 740-fold. Nevertheless, the nickase is able to induce HR at similar efficiencies as the nuclease or the homing endonuclease I–*Sce*I. Two different types of somatic HR mechanisms, recombination between tandemly arranged direct repeats as well as gene conversion using the information on an inverted repeat could be enhanced by the nickase to a similar extent as by DSB-inducing enzymes. Thus, the Cas9 nickase has the potential to become an important tool for genome engineering in plants. It should not only be applicable for HR-mediated gene targeting systems but also by the combined action of two nickases as DSB-inducing agents excluding off-target effects in homologous genomic regions.

Keywords: genome editing, targeted mutagenesis, engineered nucleases, double-strand break repair, homologous recombination, gene targeting, technical advance.

INTRODUCTION

Genome alterations in organisms that are not accessible for direct genome manipulation via homologous recombination (HR) can be achieved by introducing site-specific double-strand breaks (DSBs). This was already demonstrated in plants in the last millennium for gene targeting (GT) via HR (Puchta *et al.*, 1996) as well as gene knock-out via error-prone non-homologous end-joining (NHEJ) (Salomon and Puchta, 1998).

However, the induction of DSBs in any gene of interest requires engineered nucleases, which can be programmed to introduce breaks at any given site in the genome (Puchta and Fauser, 2013; Voytas, 2013). Currently, there are four types of engineered nucleases available for this purpose. The first class consists of modified meganucleases originating from homing endonucleases such as I–*Sce*I (Colleaux *et al.*, 1986). Although the target specificity of a meganuclease is changeable, the possible changes are highly limited (Chevalier *et al.*, 2002; Seligman *et al.*, 2002). Zinc–finger nucleases (ZFNs) were the first customisable synthetic nucleases, derived from zinc–finger proteins (Kim *et al.*, 1996). However, changing the target specificity is painstaking and not all sequences are possible targets for ZFNs. The third type, synthetic transcription activator-like effector nucleases (TALENs), is derived from the bacterial plant pathogen genus *Xanthomonas*, which offers far more options in choosing the target sequence than do ZFNs (Boch *et al.*, 2009; Moscou and Bogdanove, 2009). Nevertheless, cloning is still laborious and plasmid instabilities can occur in *Escherichia coli* as well as *Agrobacterium tumefaciens* during the cloning and

transformation procedure of new TALENs due to the repetitive structure of the DNA-binding domain.

Recently, a fourth class of engineered nucleases has become available: the CRISPR/Cas system (for 'clustered regularly interspaced short palindromic repeats'; 'CRISPR-associated'), an RNA-guided endonuclease (RGN). It originates from bacteria and archaea, in which it serves as an adaptive immune response system that degrades invading foreign plasmid or viral DNA (see Wiedenheft *et al.*, 2012 for review). The elucidation of the molecular mechanism of a type II CRISPR/Cas system from *Streptococcus pyogenes* has revealed a simple three component system (Jinek *et al.*, 2012). The protein Cas9 is a nuclease that is able to cleave double-stranded DNA with two nuclease domains (RuvC-like domain I and HNH motif), each cleaving one of the two strands. The target specificity is governed by a short CRISPR RNA (crRNA) that binds directly to a 20–nucleotide (nt) sequence on the target DNA (the so-called protospacer). An additional 3-nt element (termed protospacer-adjacent motif; PAM) with the sequence NGG downstream of the target sequence is needed for binding and cleavage by Cas9. This means that any 23-nt spanning sequence ending in GG can be targeted. The *trans*-activating CRISPR RNA (tracrRNA) interacts with the crRNA and facilitates the recruitment of the Cas9 protein and therefore the cleavage of the DNA target sequence. A direct fusion of the two RNAs to form a chimeric single-guide RNA (sgRNA) is also possible without losing cleavage activity (Jinek *et al.*, 2012). DNA cleavage occurs 3-base pairs (bp) upstream of the PAM. Because the target specificity of the nuclease is directly determined by a short sequence in the sgRNA and the Cas9 protein always stays the same, cloning of a new nuclease with altered target recognition is most likely as easy as it can get.

CRISPR/Cas nucleases have been exploited for genome manipulations in bacteria (Jiang *et al.*, 2013), human cells (Cong *et al.*, 2013; Mali *et al.*, 2013b), *C. elegans* (Friedland *et al.*, 2013), zebrafish (Hwang *et al.*, 2013), *Drosophila* (Gratz *et al.*, 2013), mice (Wang *et al.*, 2013) and even monkeys (Niu *et al.*, 2014).

A series of articles published recently demonstrates the application of CRISPR/Cas nucleases in different plant species including crop plants (Li *et al.*, 2013; Nekrasov *et al.*, 2013; Shan *et al.*, 2013; Baltes *et al.*, 2014; for review see Puchta and Fauser, 2013). In most of these studies, targeted mutagenesis was demonstrated by polymerase chain reaction (PCR) and Sanger sequencing in somatic cells. Unfortunately, until now there has been only one report published on the generation of heritable mutations in plants (Feng *et al.*, 2014), which is the most important step for biotechnological applications.

In addition to its role as a nuclease, Cas9 can also be engineered to work as a nickase that produces single-strand breaks (SSBs). This is achieved by introducing point mutations in one of the two nuclease domains (Jinek *et al.*, 2012). Instead of the error-prone repair via NHEJ, SSBs are repaired with high fidelity. This is of particular interest to avoid unwanted mutagenesis caused by off-site effects during GT experiments.

Here, we report that the nuclease, but not the nickase, can be used for efficient NHEJ-mediated mutagenesis and can be applied for the fast and efficient generation of heritable mutations in *Arabidopsis thaliana* plants by *Agrobacterium*-mediated transformation. Furthermore, we compare the efficiency of CRISPR/Cas-based nucleases and nickases to induce HR in two reporter lines bearing different recombination substrates and demonstrate that both the nickase and the nuclease are efficient tools to induce different types of HR reactions.

RESULTS

Engineering CRISPR/Cas RNA-guided nucleases and nickases

To set up a CRISPR/Cas expression system in plants we cloned the *Streptococcus pyogenes* Cas9 (SpCas9) open reading frame (ORF) that was codon-optimised for *A. thaliana* into a binary vector for *Agrobacterium*-mediated transformation. Furthermore, we cloned a Cas9 variant

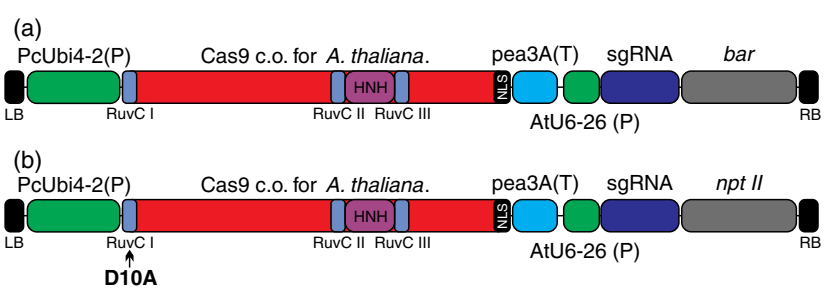

Figure 1. CRISPR/Cas expressions constructs.
Both the nuclease as well as the nickase are driven by the PcUbi4-2 promoter. Transcription is terminated by the pea3A terminator from *P. sativum*. The sgRNA is controlled by the Arabidopsis U6-26 promoter. Primary transformants can be selected due to a *bar* resistance cassette (Cas9 nuclease) (a) or an *npt II* resistance cassette (Cas9 nickase) (b). The different domain structures of Cas9 are highlighted (RuvC-like domains, HNH motif). The D10A mutation transforming the Cas9 nuclease to a nickase is located in the RuvC I domain. For detailed information see Figures S1–S5.

containing an inactivating point mutation in the catalytic residue of the RuvC-like domain (D10A), which acts as a nickase (Jinek *et al.*, 2012). Both the nuclease as well as the nickase, are driven by the constitutive Ubiquitin4–2 promoter from *Petroselinum crispum* (PcUbi4-2). The sgRNA chimera can easily be customised for any target site of interest and is under the control of the *Arabidopsis* U6-26 promoter. Figure 1 depicts the principle architecture of the T-DNA that was used in this study. The detailed design and development of our CRISPR/Cas expression system is described in the experimental procedure section.

We used this system to generate RNA-guided endonucleases (RGNs) for three endogenous target sites (*ADH1*, alcohol dehydrogenase 1, AT1G77120; *TT4*, transparent testa 4, AT5G13930; and *RTEL1*, regulator of telomere length 1, AT1G79950) as well as two HR reporter lines (DGU.US and IU.GUS).

Comparison of the efficiency of the Cas9 nuclease and nickase for targeted mutagenesis by amplicon deep sequencing

To determine the efficiency of the CRISPR/Cas nuclease and nickase to induce mutations due to error-prone NHEJ, we performed amplicon deep sequencing. An sgRNA was designed that targeted exon 2 of the *RTEL1* locus in *Arabidopsis*, and was assembled in pEn-Chimera. The sgRNA was then combined with either Cas9 or the Cas9-D10A nickase by Gateway® cloning into pDe-Cas9 or pDe-Cas9-D10A, respectively. The constructs were transformed into Arabidopsis via *Agrobacterium*-mediated transformation. Thirty primary transformants each for the nuclease and the nickase were pooled and DNA was extracted. MID-labelled (Multiplex Identifiers) PCR-amplicons covering the Cas9 protospacer were generated and sequenced on a Roche 454 system. We obtained 27 366 individual reads for the nuclease and 38 719 reads for the nickase.

For the nuclease, the number of mutations per read strongly increased at the Cas9 target site (Figure 2a). Mutations were detected in 26.7% of all reads within 4-bp from the PAM; 23.8% were insertions predominantly of a single nucleotide, and 2.8% were deletions that ranged from a single nucleotide to more than 100-nt (Figure 2b). In the case of the nickase, 14 mutations were observed at the same position, representing an over 740-fold reduction with respect to the nuclease. It is notable that these mutations are likely to be due to background noise, e.g. sequencing errors, because there is no accumulation of mutations present in the region of the protospacer.

Generating lines to identify heritable targeted mutagenesis

To determine the efficiency of heritable targeted mutagenesis events induced by the nuclease, RGNs recognising *ADH1* and *TT4* (Figure 3a) were transformed independently via floral dipping. Primary transformants (T1 generation) were selected for further cultivation in the greenhouse. Progeny of the primary transformants (T2 generation) were first checked for single locus T-DNA integration events via standard segregation analysis on selection media. Subsequently, progeny from single locus T1 plants were sown on a substrate to additionally enable the identification of mutated T2 plants that had already lost the T–DNA coding for the Cas9 expression cassette due to Mendelian segregation.

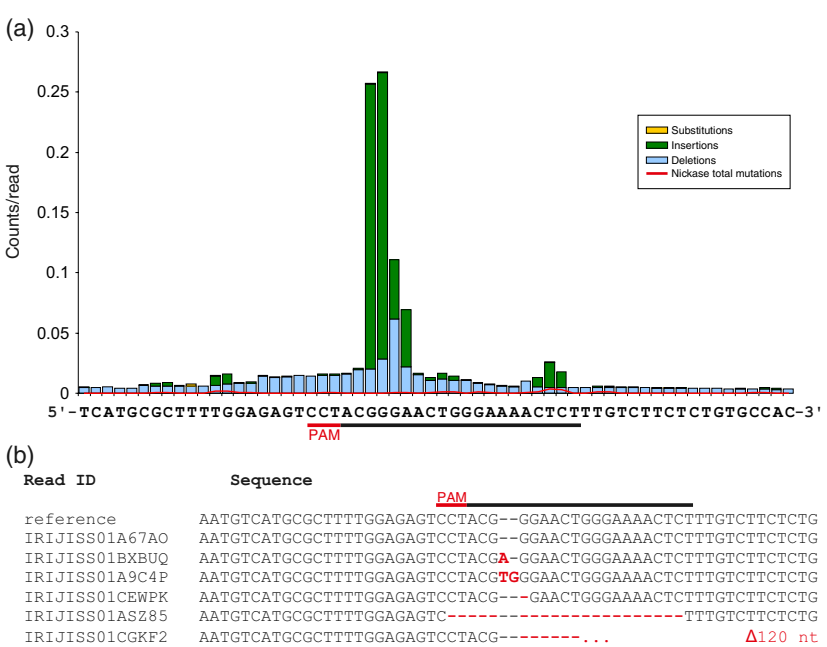

Figure 2. Deep sequencing analysis of the Cas9 nuclease and nickase.
(a) Comparison of Cas9 nuclease and nickase-induced mutations detected by amplicon deep sequencing. Depicted are the relative numbers of mutated reads as a fraction of total read numbers by sequence position. The nickase (red line) does not produce a considerable amount of mutations in the region of the protospacer. For the nuclease, the mutation frequency peaks 4-bp downstream of the PAM with 26.8% mutated reads being mostly insertions.
(b) Different types of mutations induced by the Cas9 nuclease. A number of reads represents the wild type, the most common type of mutations are insertions. Deletions can also be found, ranging from a single to more than 100 nucleotides.

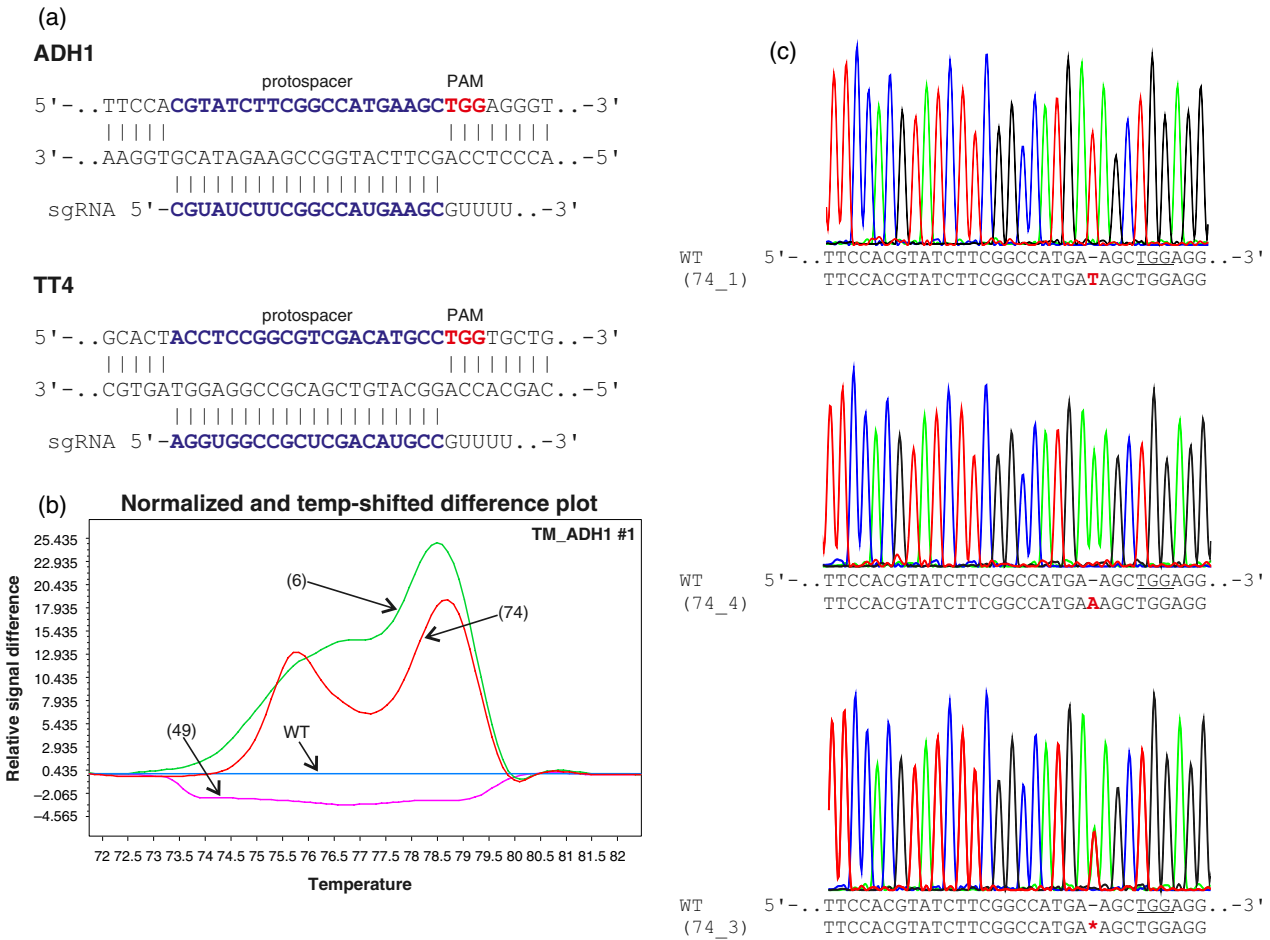

(d)

WT	5'-..CGTATCTTCGGCCATGA--AGCTGGAGGGTAATAG..-3'	
TM_ADH1 #1 (6_1)	CGTATCTTCGGCCATGAGA---------GTAATAG	Δ9/+2
TM_ADH1 #1 (49)	CGTATCTTCGGCCATGAT-AGCTGGAGGGTAATAG	+1
TM_ADH1 #1 (74_1)	CGTATCTTCGGCCATGAT-AGCTGGAGGGTAATAG	+1
TM_ADH1 #1 (74_4)	CGTATCTTCGGCCATGAA-AGCTGGAGGGTAATAG	+1
TM_ADH1 #1 (74_3)	CGTATCTTCGGCCATGA*-AGCTGGAGGGTAATAG	Heteroallelic

Figure 3. Heritable targeted mutagenesis in *ADH1* and *TT4*.
(a) Schematic of the Arabidopsis *ADH1* and *TT4* loci showing the location of the protospacer (blue) and the corresponding PAM (red). Detailed analysis of targeted mutagenesis events in T2 and T3 generations are depicted for *ADH1* (b–d).
(b) High resolution melting analysis in T2 generation of the Cas9 expression line TM_ADH1 #1 (see also Figure S7 for normalised and shifted melting curves). Depicted are a homozygous (49, purple), a heterozygous (6, green) and a transheterozygous (74, red) mutated plant. At first, we used HRM analysis to identify mutant candidates. Candidates were subsequently Sanger sequenced in T2 and T3 generation to confirm either HRM analysis (T2) or stable inheritance (T3).
(c) The transheterozygous line TM_ADH1 #1 (74) shows respective segregating patterns in T3 generation: (74_1) is homozygous for a 'T' insertion, (74_4) is homozygous for an 'A' insertion and (74_3) is again transheterozygous, indicated by an overlaid signal in the chromatogram.
(d) A subset of Sanger sequencing results of TM_ADH1 #1 (6), (49) and (74) in the T3 generation (see also Figure S8 for sequencing results of more T3 plants).

Additionally, the frequency of homozygously mutated plants in the *ADH1* locus was determined by phenotyping in the T2 generation. Therefore, progeny of seven primary transformants were subjected to allyl alcohol treatment. A functional wild type allele of *ADH1* results in the conversion of allyl alcohol to acrylaldehyde, which is highly toxic, leading to plant death (Jacobs *et al.*, 1988).

Quantification and Mendelian inheritance of heritable targeted mutagenesis events

Mutations may occur anytime during the development of T1 plants due to the constitutive expression of the Cas9 nuclease. Mutations happening early in the development of T1 plants may enter the germ line if they become

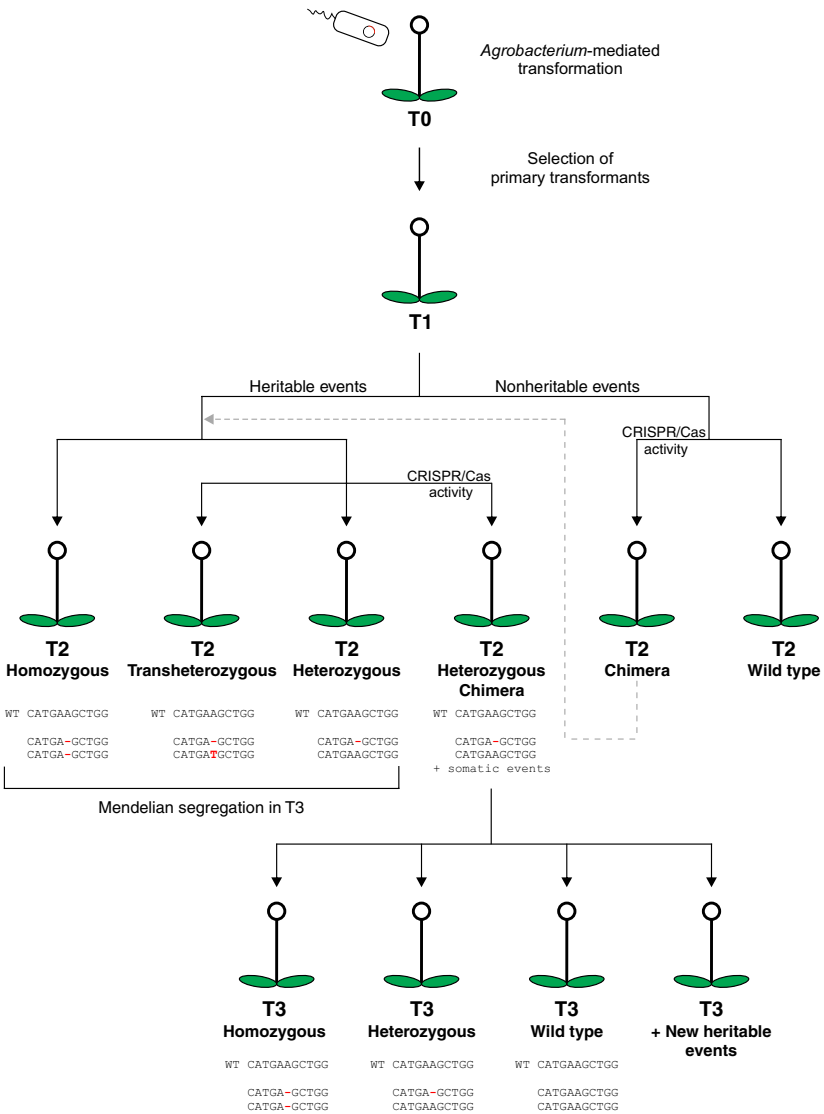

Figure 4. Schematic representation of different targeted mutagenesis outcomes in the T2 and T3 generations.
After stable *Agrobacterium*-mediated transformation, primary transformants (T1) are selected on respective selection medium. If the nuclease is active, mutations can either be inherited (left) or are lost (right). If a mutation enters the germline of a T1 plant, it may be either homozygous or heterozygous in T2. A transheterozygous genotype (heteroallelic) can be explained if different mutations occur during T1 development. Thus, these mutations may independently enter either the maternal or the paternal germline. A heterozygous plant may become a 'heterozygous chimera' if the Cas9 nuclease is actively inducing new NHEJ patterns within the wild type allele. If Cas9-induced mutations are not inherited in T1 plants respective offspring is regarded as wild type. If the Cas9 nuclease is inducing mutations in wild type T2 plants potential NHEJ patterns might arise within both wild type alleles. Therefore, respective plants are described as 'chimera'.

clonal in the shoot apical meristem. Mutations taking place later in development are most likely to be transmitted to the next generation if they occur in germinal tissues. However, as long as Cas9 is active and finds an intact recognition site, mutations may be induced at the target locus. Therefore, the genotype of analysed plants in the T2 generation can be classified into six variants (Figure 4). The most obvious variants are homozygous, heterozygous and wild type but there are also transheterozygous (heteroallelic mutations) as well as two different types of chimeras if the Cas9 nuclease is still active. On the one hand the wild type allele of a heterozygous plant may be mutated in T2 plants, but on the other hand, wild type plants may carry two intact recognition sites. If the chimeric plant is disposing clonal targeted mutagenesis events from early developmental phases, it may mimic a heritable event. Therefore, it is of utmost importance to perform a detailed analysis not only by checking the DNA sequencing chromatogram but also to test segregation of the expected mutation in the T3 generation.

We picked progeny of three primary transformants for detailed analysis of heritable targeted mutagenesis events in *ADH1*. Thus, approximately 100 seedlings per line were pre-analysed using high resolution melting (HRM) analysis. Samples showing a divergent melting curve with respect to the wild type, which is indicative of Cas9-induced mutations, were regarded as candidates for further analysis (Figure 3b). A subset of these samples was cross-checked by Sanger sequencing of the *ADH1* locus to confirm the HRM results. Thus, we performed PCRs spanning the recognition site for amplicon sequencing. Based on HRM analysis and Sanger sequencing, we found evidence of all six possible genotypes in the T2 generation, most importantly homozygosity, heterozygosity and transheterozygosity (Table S1).

To show that the induced mutations in *ADH1* were inherited in a Mendelian fashion, the segregation of these mutations was examined in the T3 generation. Therefore, the progeny of T2 plants (52 seeds) was subjected to allyl alcohol treatment. T2 plants heterozygous for the induced mutation produce a quarter of viable seeds while progeny carrying at least one wild type allele die after treatment. In contrast, homozygously as well as transheterozygously mutated T2 plants result in fully viable progeny. Deviating segregation rates (e.g., more than 25% surviving allyl alcohol treatment) may result from heterozygous T2 plants in which the Cas9 nuclease is still active, enabling inheritance of additional mutations within the wild type allele. For TM_ADH1 #1 five individuals had a 3:1 segregation ratio, and three were found to be either homozygous or transheterozygous (Table S1). To confirm these results on the sequence level, DNA was extracted from a selection of seedlings that survived allyl alcohol treatment. For example, the sequence analysis of TM_ADH1 #1 (49) revealed a homozygous mutation in T2 (+1-bp), segregation analysis of the respective progeny confirmed this result, and sequence analysis in T3 again proved the same type of mutation. Progeny of TM_ADH1 #1 (74) were also fully viable after allyl alcohol treatment. However, sequence analysis in T3 revealed two independent mutations (+1-bp, 'T' and +1-bp, 'A'), indicating a transheterozygous T2 plant. In contrast, TM_ADH1 #1 (6) was 3:1 segregating, and indeed, only one type of mutation was found in T3: a 9-bp deletion in combination with a 2-bp insertion (Δ9/+2-bp). Therefore, TM_ADH #1 (6) proves to be heterozygously mutated in T2. In total, we detected eight heritable events in TM_ADH1 #1 out of 100 individuals tested, which results in a targeted mutagenesis frequency of 8.0%. We performed analogues experiments for two other lines with frequencies of 15.3 and 18.2%, which equals a mean value of 13.8% of stably inherited mutant plants for *ADH1* (Table 1, see Figures S7–S12 for details). To determine a more precise frequency of targeted mutagenesis, we subjected approximately 11 000 seeds of seven independent primary transformants to allyl alcohol treatment. The number of allyl alcohol resistant seedlings was determined, and a subset of 53 T2 plants was confirmed on the sequence level (Figure S12). Taken together, 15.3% of T2 plants were found to be homozygously or transheterozygously mutated in *ADH1* (Table 1).

Similar to *ADH1*-targeted mutagenesis, mutagenesis was analysed in *TT4* and yielded comparable targeted mutagenesis frequencies. The detailed analysis is shown in the Supporting Information (Table S2 and Figures S13–S16). Overall, the progeny of three primary transformants was analysed using HRM analysis, Sanger sequencing and phenotyping in the T2 and T3 generations. We obtained heritable mutation frequencies between 2.5 and 70.0%, which equals a mean value of 28.3% for *TT4* (Table 1).

Comparison of the efficiency of Cas9 nuclease and nickase for induction of homologous recombination

To compare the ability of the CRISPR/Cas nuclease and nickase to induce HR, we tested the system in two plant HR reporter lines: DGU.US and IU.GUS (Orel *et al.*, 2003; Figure 5a). Both harbour a stably integrated, homozygous reporter construct that can be used to visualise somatic HR pathways based on the activity of β-glucuronidase (*uidA*, GUS). The GUS-ORF is disrupted by a short spacer sequence that contains a recognition site for the homing endonuclease I–*Sce*I and is therefore not functional. Upon the induction of a DSB, the ORF can be restored in DGU.US by a recombination reaction between the directly repeated sequences, as classically described by the

Table 1 Heritable targeted mutagenesis in ADH1 and TT4

Target	Plant line	Type of analysis in T2	Plants tested	Heritable events	TM frequency (%)
ADH1	TM_ADH1 #1	HRM, Sanger sequencing	100	8	8
	TM_ADH1 #2		98	15	15.3
	TM_ADH1 #3		99	18	18.2
			297	41	13.8
TT4	TM_TT4 #1	HRM, Sanger sequencing	40	1	2.5
	TM_TT4 #2		40	5	12.5
	TM_TT4 #3		40	28	70
			120	34	28.3
ADH1	TM_ADH1 #4	Survival of allyl alcohol treatment	2541	355	14
	TM_ADH1 #5		1355	142	10.4
	TM_ADH1 #6		1771	167	9.4
	TM_ADH1 #7		1166	351	30.1
	TM_ADH1 #8		1340	37	2.8
	TM_ADH1 #9		1458	249	17.1
	TM_ADH1 #10		1363	383	28.1
			10 994	1685	15.3

Detailed information is given in the SI (Table S1 and S2). See Figure S6 for a schema of all plant lines that were used to identify heritable targeted mutagenesis events in either *ADH1* or *TT4.*

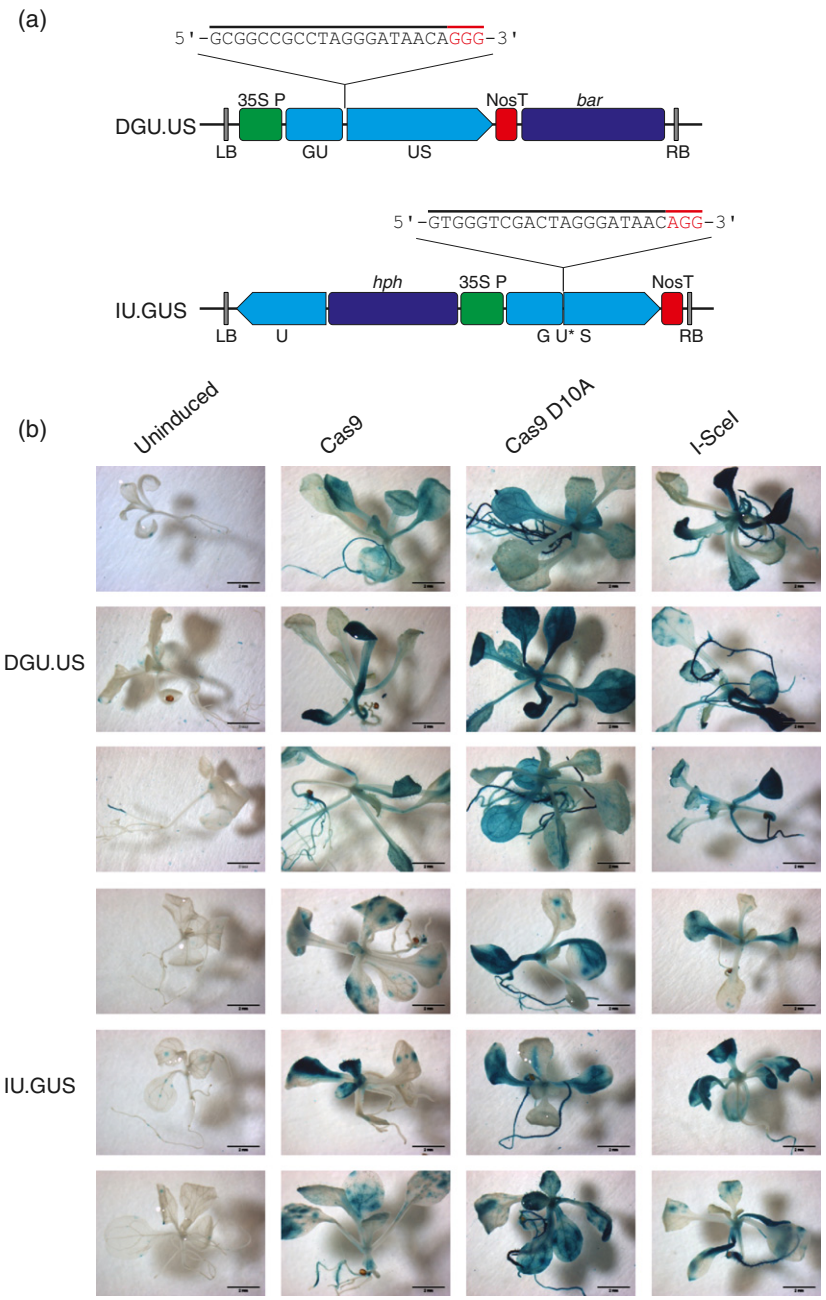

Figure 5. Induction of HR in respective reporter lines assayed by histochemical staining.
(a) HR reporter constructs and respective CRISPR protospacers. Induction of a DSB at the indicated target sites leads to the restoration of the GUS-ORF either by SSA (in DGU.US) or SDSA (in IU.GUS).
(b) Representative selection of stained plants. Induction with Cas9 nuclease or nickase (D10A) leads to a strong increase of blue areas in both reporter lines.

single-strand annealing (SSA) model or in IU.GUS by a gene conversion using an inverted homologous sequence, as classically described by the synthesis-dependant strand annealing (SDSA) model. The restored gene can be visualised by staining with the artificial substrate X-Glc (Figure 5a).

We designed and cloned Cas9 nucleases and nickases that recognised the interrupting sequence in each of the reporter lines. Since the DGU.US reporter construct carried a *bar* gene, the resistance gene for the respective nuclease was changed to *npt* II. The constructs were transformed into the respective reporter line via floral dipping. For comparison, an I-*Sce*I expression construct that has been described before (Fauser *et al.*, 2012) was also transformed as a positive control. T1 transformants were selected and stained with X-Glc. In all cases, we obtained plants with huge stained areas in contrast to only several small sectors on the control plants without DSB induction, indicating that both HR pathways can be efficiently induced by CRISPR/Cas nucleases or nickases (Figure 5b).

To quantify and compare the HR inducing potential of the different enzymes, a fluorescent assay using 4-methyl-umbelliferyl-β-D-glucuronide (4-MUG) was applied (Gould and Smith, 1989). 4-MUG can be converted to the

fluorescent 4-methylumbelliferone (4-MU) by the GUS enzyme. For each plant line, 10 T1 plants were selected after 2 weeks of growth and were incubated with 4-MUG. This was conducted three times for all lines. For all three systems (I-*Sce*I, Cas9 nuclease, Cas9 nickase) fluorescence was higher in the DGU.US line than with the IU.GUS reporter (Figure 6). This is consistent with the results obtained in previous studies using these reporter constructs (Orel *et al.*, 2003; Mannuss *et al.*, 2010; Roth *et al.*, 2012). Additionally, in all cases, the lines harbouring a nuclease or nickase showed a much higher fluorescence than the uninduced control lines and the wild type line. In both DGU.US and IU.GUS the induction achieved by the CRISPR/Cas nuclease was only little lower than for I-*Sce*I. Surprisingly, the application of the nickases resulted in the highest induction in both reporter lines, indicating that the nickases are able to induce HR at least as good as I-*Sce*I.

Thus, our data clearly demonstrate that whereas the CRISPR/Cas nuclease can be efficiently used for NHEJ-mediated mutagenesis, both the nuclease and the nickase can be used for efficient induction of HR in *A. thaliana.*

DISCUSSION

The induction of DSBs to induce changes in the genome via NHEJ or HR has become a key technology in genome engineering. A breakthrough for the application of such technologies was the development of engineered nucleases that can be adapted to any target site of interest. Engineered meganucleases, ZFNs and TALENs became available to the community over the years. Synthetic DNA-binding domains derived from zinc-finger transcription factors or transcription activator-like effectors have especially boosted the practical application of engineered nucleases in several different species. Recently, the CRISPR/Cas system became the newcomer of the engineered nucleases, offering some unique features such as an extremely efficient and simple customisation process that, in principle, can target any site of interest as well as the most cost-effective cloning. Engineered nucleases have recently been reviewed (Pauwels *et al.*, 2013; Puchta and Fauser, 2013; Voytas, 2013; Carroll, 2014).

Here we report that the CRISPR/Cas nickase may be used efficiently to induce HR and that the nuclease leads to inherited targeted mutagenesis events in the model plant *Arabidopsis.* While preparing this manuscript an independent study was published by the Jian-Kang Zhu group that also demonstrates inheritance of targeted mutagenesis events in *Arabidopsis.* Frequencies of approximately 22% homozygously mutated plants in T2 could be observed using hSpCas9 controlled by the CaMV 35S promoter (Feng *et al.*, 2014). In our approach, using codon-optimised Cas9 under the control of a plant-specific PcUbi4-2 promoter, we achieved frequencies of up to two-thirds of all plants tested. Notably, we did not analyse Cas9 activity in T1 plants, e.g., via T7 surveyor assays or diagnostic digests, that are used for analysis of heritable targeted

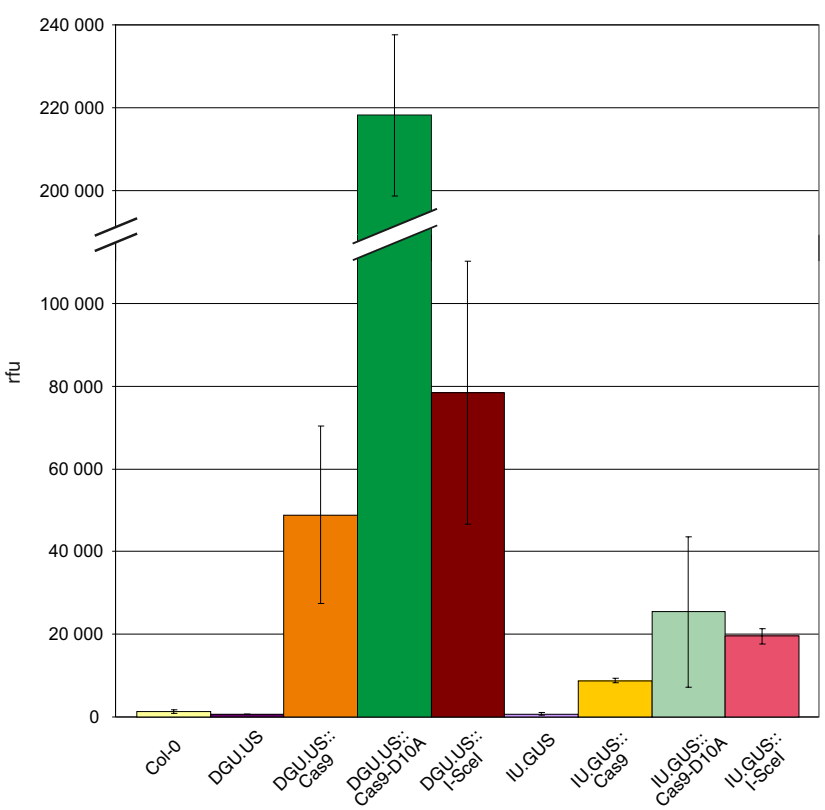

Figure 6. Quantification of HR assessed by fluorescent assay.
HR is determined by activity of restored GUS gene in the reporter lines DGU.US and IU.GUS. Activity of both reporters is shown without induction and with induction by either Cas9 nuclease, nickase (D10A) or I-*Sce*I.

mutagenesis. Instead, T1 plants were selected randomly for the detection of heritable targeted mutagenesis events in their offspring. Furthermore, we did not process every plant that showed a divergent melting curve in HRM analysis, thereby excluding them from calculation of targeted mutagenesis frequencies. Thus, our data support the applicability of the CRISPR/Cas system for efficient heritable site-directed mutagenesis in plants. Mutations are mostly small insertions and deletions leading to frameshifts that can easily be identified using routine high-throughput genotyping methods such as HRM analysis.

Most importantly, we show here the application of a CRISPR/Cas nickase in plants. By deep sequencing analysis, we clearly demonstrate that, in contrast with the nuclease, the nickase does not induce NHEJ-mediated targeted mutagenesis. We quantified the activity of CRISPR/Cas-based nucleases and nickases in two well established HR reporter lines for SSA and SDSA (Orel *et al.*, 2003; Roth *et al.*, 2012). Remarkably, for both, the nickase was able to induce HR to a similar extent as the Cas9 nuclease or the homing endonuclease I–*Sce*I. This finding shifts the focus of interest to single-stranded DNA breaks for basic research as well as for HR-mediated genome engineering. It has recently been shown in mammalian cells that there is an additional pathway for HR-mediated repair of SSBs that is distinct from DSB repair (Davis and Maizels, 2014). This pathway is associated with transcription and is most efficient when the SSB is located on the transcribed strand. Indeed, the nickases used in this study for HR analysis nicked the transcribed strand within the spacer region in the GUS gene. Upcoming studies will show whether this strand-dependant difference can also be observed in plants. This may most reasonably be analysed in transient test systems, such as those that have been recently described for the quantification of the cleavage efficiencies of engineered nucleases (Johnson *et al.*, 2013). Moreover, Cas9 nickases may generally be used to characterise HR-mediated SSB repair pathways in plants by epistasis analysis in different mutant backgrounds, as we have previously performed for DSB repair (Mannuss *et al.*, 2010; Roth *et al.*, 2012).

Cas9 nickases may also enhance the toolbox for genome engineering approaches. Because of the widespread occurrence of duplications in plant genomes, the number of Cas9 nuclease target sites at certain loci might be limited due to the presence of ectopic sequences that are almost or even completely identical. To extend the use of CRISPR/Cas to respective target sites Cas9 may be applied as paired nickases resulting in a DSB-inducing agent that doubles the recognition site from 20 to 40-nts. This may also reduce the risk of off-target activity by Cas9 nucleases. Paired Cas9 nickases have been shown previously to induce targeted mutagenesis in mammalian cells (Mali *et al.*, 2013a; Ran *et al.*, 2013) and it will be important to test the applicability of this concept also in plants. Furthermore, the potential of Cas9 nickases to induce HR opens the possibility of using the system for GT experiments. We were able to demonstrate that GT frequencies are strongly enhanced by DSB induction at the target site (Puchta *et al.*, 1996). More recently, we developed the *in planta* GT system, which is based on simultaneous DSB induction (Fauser *et al.*, 2012). Future experiments may show if these systems can also be triggered by SSB induction. For simultaneous DSB or SSB induction, Cas9 is able to handle the presence of multiple sgRNAs, allowing for the recognition of several target sites at once.

Taken together, we were able to demonstrate the fast and efficient generation of stable mutants using our CRISPR/Cas system. Moreover, we were able to apply the Cas9 nickase to plants, showing that the nickase does indeed not induce NHEJ but exclusively HR at a similar efficiency to DSB-inducing agents.

EXPERIMENTAL PROCEDURES

Strains

All lines used in this study are on a Columbia-0 background. Seeds were sown on agar plates containing germination medium (GM) or on substrate containing 1:1 Floraton 3 (Floragard Vertriebs GmbH, www.floragard.de, Oldenburg, Germany) and Vermiculite (Deutsche Vermiculite Dämmstoff GmbH, www.vermiculite.de, Sprockhövel, Germany).

T-DNA constructs

The backbone of the binary vectors used in this study was derived from pPZP201 (Hajdukiewicz *et al.*, 1994) and was further optimised. First, the multiple cloning site was modified to provide more restrictions sites between *Eco*RI and *Bam*HI. Therefore, oligos SBO-1 and SBO-2 (see Table S3 for a list of all oligos used in this study) were annealed and cloned between the *Eco*RI and *Bam*HI sites of pPZP201, yielding in pSBO-1. Second, a *bar* resistance cassette for the selection of successfully transformed plants was transferred from pGU.C.US.B (Siebert, 2002) via *Hind*III to pSBO-1, resulting in pSBO-2.

To create a Cas9 expression cassette the pea3A terminator from *Pisum sativum* was amplified using pFZ19 (Addgene plasmid 36184, Zhang *et al.*, 2010) as a template with primers SS-34/SS-35 including *Sac*I overhangs. The amplicon was cloned into the *Sac*I site of pSBO-2 to generate pCAS9-T. Subsequently, the PcUbi4-2 promoter was amplified using pPZP221-Ubi::I-SceI (Fauser *et al.*, 2012) as a template with primers SS-32/SS-33 including *Eco*RI overhangs. The amplicon was cloned into the *Eco*RI site of pCAS9-T to generate pCAS9–TP. The Cas9 ORF was codon-optimised for *A. thaliana* and assembled by GeneArt® (Life Technologies Inc., www.lifetech.com, Carlsbad, CA, USA) flanked by *Asc*I recognition sites for further subcloning into pCAS9-TP to generate pCAS9-TPC. The general architecture of our Cas9 ORF is based on the version that was developed by the group of George M. Church, which bears a SV40 nuclear localisation signal at the C-terminal end (Mali *et al.*, 2013b).

The customisable RNA chimera is driven by the Arabidopsis U6-26 promoter (Waibel and Filipowicz, 1990; Li and Jiang, 2007) and was also synthesised by GeneArt® flanked by *Avr*II sites, resulting in the vector pChimera. To specify the chimera for the respective target sequence, pChimera was linearised using *Bbs*I,

and the spacer was ligated between the two *Bbs*I sites using annealed oligonucleotides. The customised RNA chimera was then transferred into pCAS9-TPC via *Avr*II to obtain a functional Cas9 expression construct for targeted mutagenesis. Respective expression constructs were used for targeted mutagenesis in *ADH1* and *TT4*. For *ADH1* oligos FF-188/FF-189 were annealed and cloned into the *Bbs*I sites of pChimera. Likewise, oligos FF-190/FF-191 were used for *TT4*.

Compatible versions of pCAS9-TPC and pChimera for Gateway® cloning (Life Technologies Inc.) were also cloned: pDe-CAS9 and pEn-Chimera. For pDe-CAS9 a PCR-amplified Gateway® destination cassette was added that contained attL1/2 sites and a *ccdB* gene via *Avr*II. The U6-26 promoter and the sgRNA were amplified together by PCR from pChimera using attR1/2 containing primers (SS-40/SS-41), and the amplicon was TA-cloned into the pGEM®-T Easy vector (Promega Corp., www.promega.com), resulting in pEn-Chimera. The CRISPR spacer can be introduced into pEn-Chimera using *Bbs*I as described for pChimera. The customised RNA chimera is then transferred into pDe–CAS9 by a single site Gateway® LR reaction. The Gateway®-compatible system allows target site selection incorporating *Avr*II recognition sites and simplifies the cloning procedure.

The Cas9 nickase was made via PCR-based site-directed mutagenesis with primers SS-98/SS-99, which harbour the desired single nucleotide exchange using pCAS9-TPC as template creating pCAS9-D10A. The *bar* resistance cassette was exchanged via *Hind*III with a kanamycin resistance cassette (*npt* II) generated by PCR from pPZP111 (Hajdukiewicz *et al.*, 1994) using primers SS-30/SS-31. The same approach was made to exchange the resistance cassette for the DGU.US nuclease construct. Similar to pCAS9-TPC a destination construct for Gateway® cloning was added to the nickase vector via *Avr*II, creating pDe-CAS9-D10A.

Sequence information is given in the SI (Figures S1–S5). The Cas9 expression systems developed in this study (pCAS9-TPC, pChimera, pDe-CAS9, pEn-Chimera, pDe-CAS9-D10A) are available on request.

Plant transformation

Arabidopsis plants were transformed via *Agrobacterium*-mediated transformation as described previously (Clough and Bent, 1998).

Analysis of beta-glucoronidase activity

For a general impression of the Cas9 activity conventional GUS staining was performed as described previously (Orel *et al.*, 2003) 10–14 days after seeds were sown on GM plates containing selection marker and cefotaxim.

The exact quantification was performed using a 4-MUG assay (Gould and Smith, 1989). For each line, T1 seeds were sown on GM containing the appropriate selection marker (phosphinothricin or kanamycin). After 2 weeks of incubation, 10 plants were harvested and submerged in 10 ml of GUS extraction buffer (50 mM sodium phosphate, 10 mM EDTA, 0.1% SDS and 0.1% Triton X-100) containing 1 mM 4–MUG and incubated at room temperature. At given time points, 100 μl was taken from the reaction, and 50 μl of stop reagent (1 M sodium carbonate) was added. Measurement was performed in an EnSpire® Multimode Plate Reader (PerkinElmer Inc., www.perkinelmer.com, Waltham, MA, USA) with excitation at 365 nm and emission at 455 nm.

Amplicon deep sequencing

T1 plants were grown on GM with respective selection markers. DNA was extracted from batches of 30 plants after 2 weeks of incubation as described (Salomon and Puchta, 1998). MID-labelled amplicons were generated using a proof-reading polymerase with 100 ng of genomic DNA using primers SS-145 to SS-150 and purified using the Roche High Pure PCR Product Purification Kit. Roche 454 sequencing was performed by Eurofins MWG Operon (MWG Eurofins GmbH, www.eurofinsgenomics.eu). Data analysis was performed using the Galaxy web server (Giardine *et al.*, 2005; Blankenberg *et al.*, 2010; Goecks *et al.*, 2010) and INTEGRATIVE GENOMICS VIEWER 2.3 (Robinson *et al.*, 2011; Thorvaldsdóttir *et al.*, 2013).

Evaluation of germinal mutations

Primary transformants (T1) were selected on agar plates containing GM, phosphinothricin and cefotaxim for further cultivation in the greenhouse. Progeny (T2) were checked for a 3:1 segregation on selection media to identify single locus lines. Single locus lines (T2) were sown on substrate to identify heritable targeted mutagenesis events via HRM analysis (see Figure S6). HRM analysis were performed using the Roche LightCycler® 480 2.0 system (Roche Diagnostics International AG, www.roche-diagnostics.us, Rotkreuz, Switzerland), the Roche LightCycler® 480 High Resolution Melting Master reaction mix and the Roche LightCycler® 480 Gene Scanning Software. Genomic DNA was extracted from approximately 14-day-old T2 seedlings. To genotype *ADH1* lines, primers FF-62/FF-63 were used. Likewise, we used primers JS-58/JS-59 to genotype *TT4* lines. Plants showing a divergent melting curve were regarded as mutated, and mutations were confirmed via Sanger sequencing in the T2 as well as the T3 generation (GATC Biotech AG, www.gatc-biotech.com, Konstanz, Germany). The *ADH1* locus was PCR-amplified using primers FF-227/FF-228 and sequenced using FF-227. Likewise, the *TT4* locus was PCR-amplified using primers oFZ3/oFZ4 and sequenced using oFZ3.

Mendelian inheritance of mutations was examined in the T3 generation by phenotyping as well as by Sanger sequencing of PCR products spanning the target sequence.

ACKNOWLEDGEMENTS

We thank Maren Scheidle, Hanna Hiller, Laura Giese, Simon Stowasser and Waltraud Wehrle for excellent technical assistance and Julian Röhrig for assisting with the PlateReader. This work was funded by the European Research Council (Advanced Grant 'COMREC').

SUPPORTING INFORMATION

Additional Supporting Information may be found in the online version of this article.

Figure S1. Sequence information for pCAS9-TPC.
Figure S2. Sequence information for pDe-CAS9.
Figure S3. Sequence information for pDe-CAS9-D10A.
Figure S4. Sequence information for pChimera.
Figure S5. Sequence information for pEn-Chimera.
Figure S6. Summary of all lines used for targeted mutagenesis in ADH1 and TT4.
Figure S7. Detailed analysis of targeted mutagenesis events using the CRIPSR/Cas expression line TM_ADH1 #1.
Figure S8. Sanger sequencing results of targeted mutagenesis events derived from TM_ADH1 #1.
Figure S9. Sanger sequencing results of targeted mutagenesis events derived from TM_ADH1 #2.
Figure S10. Sanger sequencing results of targeted mutagenesis events derived from TM_ADH1 #3.
Figure S11. Phenotypes of mutants obtained from successful targeted mutagenesis events.
Figure S12. Sanger sequencing results of targeted mutagenesis events derived from TM_ADH1 #4 to TM_ADH1 #10.

Figure S13. Sanger sequencing results of targeted mutagenesis events derived from TM_TT4 #1.
Figure S14. Sanger sequencing results of targeted mutagenesis events derived from TM_TT4 #2.
Figure S15. Sanger sequencing results of targeted mutagenesis events derived from TM_TT4 #3 (T2 Generation).
Figure S16. Sanger sequencing results of targeted mutagenesis events derived from TM_TT4 #3 (T3 Generation).
Table S1. Heritable targeted mutagenesis in ADH1.
Table S2. Heritable targeted mutagenesis in TT4.
Table S3. Oligos used in this study.

REFERENCES

Baltes, N.J., Gil-Humanes, J., Cermak, T., Atkins, P.A. and Voytas, D.F. (2014) DNA replicons for plant genome engineering. *Plant Cell*, **26**, 151–163.

Blankenberg, D., Von Kuster, G., Coraor, N., Ananda, G., Lazarus, R., Mangan, M., Nekrutenko, A. and Taylor, J. (2010) Galaxy: a web-based genome analysis tool for experimentalists. *Curr. Protoc. Mol. Biol.* **Chapter 19**, Unit 19.10.1–21.

Boch, J., Scholze, H., Schornack, S., Landgraf, A., Hahn, S., Kay, S., Lahaye, T., Nickstadt, A. and Bonas, U. (2009) Breaking the code of DNA binding specificity of TAL-type III effectors. *Science*, **326**, 1509–1512.

Carroll, D. (2014) Genome engineering with targetable nucleases. *Annu. Rev. Biochem.* doi: 10.1146/annurev-biochem-060713-035418.

Chevalier, B.S., Kortemme, T., Chadsey, M.S., Baker, D., Monnat, R.J. and Stoddard, B.L. (2002) Design, activity, and structure of a highly specific artificial endonuclease. *Mol. Cell*, **10**, 895–905.

Clough, S.J. and Bent, A.F. (1998) Floral dip: a simplified method for *Agrobacterium*-mediated transformation of *Arabidopsis thaliana*. *Plant J.* **16**, 735–743.

Colleaux, L., d'Auriol, L., Betermier, M., Cottarel, G., Jacquier, A., Galibert, F. and Dujon, B. (1986) Universal code equivalent of a yeast mitochondrial intron reading frame is expressed into *E. coli* as a specific double strand endonuclease. *Cell*, **44**, 521–533.

Cong, L., Ran, F.A., Cox, D. *et al.* (2013) Multiplex genome engineering using CRISPR/Cas systems. *Science*, **339**, 819–823.

Davis, L. and Maizels, N. (2014) Homology-directed repair of DNA nicks via pathways distinct from canonical double-strand break repair. *Proc. Natl Acad. Sci. USA*, **111**, E924–E932.

Fauser, F., Roth, N., Pacher, M., Ilg, G., Sánchez-Fernández, R., Biesgen, C. and Puchta, H. (2012) *In planta* gene targeting. *Proc. Natl Acad. Sci. USA*, **109**, 7535–7540.

Feng, Z., Mao, Y., Xu, N. *et al.* (2014) Multigeneration analysis reveals the inheritance, specificity, and patterns of CRISPR/Cas-induced gene modifications in *Arabidopsis*. *Proc. Natl Acad. Sci. USA*, **111**, 4632–4637.

Friedland, A.E., Tzur, Y.B., Esvelt, K.M., Colaiácovo, M.P., Church, G.M. and Calarco, J.A. (2013) Heritable genome editing in *C. elegans* via a CRISPR-Cas9 system. *Nat. Methods*, **10**, 741–743.

Giardine, B., Riemer, C., Hardison, R.C. *et al.* (2005) Galaxy: a platform for interactive large-scale genome analysis. *Genome Res.* **15**, 1451–1455.

Goecks, J., Nekrutenko, A. and Taylor, J. (2010) Galaxy: a comprehensive approach for supporting accessible, reproducible, and transparent computational research in the life sciences. *Genome Biol.* **11**, R86.

Gould, J.H. and Smith, R.H. (1989) A non-destructive assay for GUS in the media of plant tissue cultures. *Plant Mol. Biol. Report.* **7**, 209–216.

Gratz, S.J., Cummings, A.M., Nguyen, J.N., Hamm, D.C., Donohue, L.K., Harrison, M.M., Wildonger, J. and O'Connor-Giles, K.M. (2013) Genome engineering of *Drosophila* with the CRISPR RNA-guided Cas9 nuclease. *Genetics*, **194**, 1029–1035.

Hajdukiewicz, P., Svab, Z. and Maliga, P. (1994) The small, versatile pPZP family of *Agrobacterium* binary vectors for plant transformation. *Plant Mol. Biol.* **25**, 989–994.

Hwang, W.Y., Fu, Y., Reyon, D., Maeder, M.L., Tsai, S.Q., Sander, J.D., Peterson, R.T., Yeh, J.-R.J. and Joung, J.K. (2013) Efficient genome editing in zebrafish using a CRISPR-Cas system. *Nat. Biotechnol.* **31**, 227–229.

Jacobs, M., Dolferus, R. and Van den Bossche, D. (1988) Isolation and biochemical analysis of ethyl methanesulfonate-induced alcohol dehydrogenase null mutants of *Arabidopsis thaliana* (L.) Heynh. *Biochem. Genet.* **26**, 105–122.

Jiang, W., Bikard, D., Cox, D., Zhang, F. and Marraffini, L.A. (2013) RNA-guided editing of bacterial genomes using CRISPR-Cas systems. *Nat. Biotechnol.* **31**, 233–239.

Jinek, M., Chylinski, K., Fonfara, I. and Hauer, M. (2012) A programmable dual-RNA–guided DNA endonuclease in adaptive bacterial immunity. *Science*, **337**, 816–821.

Johnson, R.A., Gurevich, V. and Levy, A.A. (2013) A rapid assay to quantify the cleavage efficiency of custom-designed nucleases *in planta*. *Plant Mol. Biol.* **82**, 207–221.

Kim, Y.G., Cha, J. and Chandrasegaran, S. (1996) Hybrid restriction enzymes: zinc finger fusions to Fok I cleavage domain. *Proc. Natl Acad. Sci. USA*, **93**, 1156–1160.

Li, X. and Jiang, D. (2007) Varied transcriptional efficiencies of multiple *Arabidopsis* U6 small nuclear RNA genes. *J. Integr. Plant Biol.* **49**, 222–229.

Li, J.-F., Norville, J.E., Aach, J., McCormack, M., Zhang, D., Bush, J., Church, G.M. and Sheen, J. (2013) Multiplex and homologous recombination-mediated genome editing in *Arabidopsis* and *Nicotiana benthamiana* using guide RNA and Cas9. *Nat. Biotechnol.* **31**, 688–691.

Mali, P., Aach, J., Stranges, P.B., Esvelt, K.M., Moosburner, M., Kosuri, S., Yang, L. and Church, G.M. (2013a) CAS9 transcriptional activators for target specificity screening and paired nickases for cooperative genome engineering. *Nat. Biotechnol.* **31**, 833–838.

Mali, P., Yang, L., Esvelt, K.M., Aach, J., Guell, M., DiCarlo, J.E., Norville, J.E. and Church, G.M. (2013b) RNA-guided human genome engineering via Cas9. *Science*, **339**, 823–826.

Mannuss, A., Dukowic-Schulze, S., Suer, S., Hartung, F., Pacher, M. and Puchta, H. (2010) RAD5A, RECQ4A, and MUS81 have specific functions in homologous recombination and define different pathways of DNA repair in *Arabidopsis thaliana*. *Plant Cell*, **22**, 3318–3330.

Moscou, M. and Bogdanove, A. (2009) A simple cipher governs DNA recognition by TAL effectors. *Science*, **326**, 1501.

Nekrasov, V., Staskawicz, B., Weigel, D., Jones, J.D.G. and Kamoun, S. (2013) Targeted mutagenesis in the model plant *Nicotiana benthamiana* using Cas9 RNA-guided endonuclease. *Nat. Biotechnol.* **31**, 691–693.

Niu, Y., Shen, B., Cui, Y. *et al.* (2014) Generation of gene-modified cynomolgus monkey via Cas9/RNA-mediated gene targeting in one-cell embryos. *Cell*, **156**, 1–8.

Orel, N., Kyryk, A. and Puchta, H. (2003) Different pathways of homologous recombination are used for the repair of double-strand breaks within tandemly arranged sequences in the plant genome. *Plant J.* **35**, 604–612.

Pauwels, K., Podevin, N., Breyer, D., Carroll, D. and Herman, P. (2013) Engineering nucleases for gene targeting: safety and regulatory considerations. *N. Biotechnol.* **31**, 18–27.

Puchta, H. and Fauser, F. (2013) Synthetic nucleases for genome engineering in plants: prospects for a bright future. *Plant J.* doi: 10.1111/tpj.12338.

Puchta, H., Dujon, B. and Hohn, B. (1996) Two different but related mechanisms are used in plants for the repair of genomic double-strand breaks by homologous recombination. *Proc. Natl Acad. Sci. USA*, **93**, 5055–5060.

Ran, F.A., Hsu, P.D., Lin, C.-Y. *et al.* (2013) Double nicking by RNA-guided CRISPR Cas9 for enhanced genome editing specificity. *Cell*, **154**, 1380–1389.

Robinson, J.T., Thorvaldsdóttir, H., Winckler, W., Guttman, M., Lander, E.S., Getz, G. and Mesirov, J.P. (2011) Integrative genomics viewer. *Nat. Biotechnol.* **29**, 24–26.

Roth, N., Klimesch, J., Dukowic-Schulze, S., Pacher, M., Mannuss, A. and Puchta, H. (2012) The requirement for recombination factors differs considerably between different pathways of homologous double-strand break repair in somatic plant cells. *Plant J.* **72**, 781–790.

Salomon, S. and Puchta, H. (1998) Capture of genomic and T-DNA sequences during double-strand break repair in somatic plant cells. *EMBO J.* **17**, 6086–6095.

Seligman, L.M., Chisholm, K.M., Chevalier, B.S., Chadsey, M.S., Edwards, S.T., Savage, J.H. and Veillet, A.L. (2002) Mutations altering the cleavage specificity of a homing endonuclease. *Nucleic Acids Res.* **30**, 3870–3879.

Shan, Q., Wang, Y., Li, J. *et al.* (2013) Targeted genome modification of crop plants using a CRISPR-Cas system. *Nat. Biotechnol.* **31**, 686–688.

Siebert, R. (2002) Efficient repair of genomic double-strand breaks by homologous recombination between directly repeated sequences in the plant genome. *Plant Cell Online*, **14**, 1121–1131.

Thorvaldsdóttir, H., Robinson, J.T. and Mesirov, J.P. (2013) Integrative Genomics Viewer (IGV): high-performance genomics data visualization and exploration. *Brief. Bioinform.* **14**, 178–192.

Voytas, D.F. (2013) Plant genome engineering with sequence-specific nucleases. *Annu. Rev. Plant Biol.* **64**, 327–350.

Waibel, F. and Filipowicz, W. (1990) RNA-polymerase specificity of transcription of *Arabidopsis* U snRNA genes determined by promoter element spacing. *Nature*, **346**, 199–202.

Wang, H., Yang, H., Shivalila, C.S., Dawlaty, M.M., Cheng, A.W., Zhang, F. and Jaenisch, R. (2013) One-step generation of mice carrying mutations in multiple genes by CRISPR/Cas-mediated genome engineering. *Cell*, **153**, 910–918.

Wiedenheft, B., Sternberg, S.H. and Doudna, J.A. (2012) RNA-guided genetic silencing systems in bacteria and archaea. *Nature*, **482**, 331–338.

Zhang, F., Maeder, M.L., Unger-Wallace, E. *et al.* (2010) High frequency targeted mutagenesis in *Arabidopsis thaliana* using zinc finger nucleases. *Proc. Natl Acad. Sci. USA*, **107**, 12028–12033.

